Temperature chaos in 3D Ising spin glasses is driven by rare events

2013 EPL 103 67003

(http://iopscience.iop.org/0295-5075/103/6/67003)

A Letters Journal Exploring the Frontiers of Physics

September 2013

EPL, **103** (2013) 67003 www.epljournal.org
doi: 10.1209/0295-5075/103/67003

Temperature chaos in 3D Ising spin glasses is driven by rare events

L. A. Fernandez[1,2], V. Martin-Mayor[1,2], G. Parisi[3,4] and B. Seoane[3,2]

[1] *Departamento de Física Teórica I, Universidad Complutense - 28040 Madrid, Spain, EU*
[2] *Instituto de Biocomputación and Física de Sistemas Complejos (BIFI) - 50009 Zaragoza, Spain, EU*
[3] *Dipartimento di Fisica, Sapienza Università di Roma - Roma, Italy, EU*
[4] *INFN, Sezione di Roma I, IPFC-CNR - P.le A. Moro 2, I-00185 Roma, Italy, EU*

received 10 July 2013; accepted in final form 14 September 2013
published online 7 October 2013

PACS 75.50.Lk – Spin glasses and other random magnets
PACS 75.40.Mg – Numerical simulation studies

Abstract – Temperature chaos has often been reported in the literature as a rare-event–driven phenomenon. However, this fact has always been ignored in the data analysis, thus erasing the signal of the chaotic behavior (still rare in the sizes achieved) and leading to an overall picture of a weak and gradual phenomenon. On the contrary, our analysis relies on a large-deviations functional that allows to discuss the size dependences. In addition, we had at our disposal unprecedentedly large configurations equilibrated at low temperatures, thanks to the Janus computer. According to our results, when temperature chaos occurs its effects are strong and can be felt even at short distances.

Temperature chaos (TC) refers to the complete reorganization of the equilibrium configurations by the slightest change in temperature. This effect was initially predicted in spin glasses (SG) [1–3] but it is expected as well in other glassy materials such as polymers [4,5] or vortex glasses [6].

An experimental measurement of TC is still missing. The main difficulty arises from the non-equilibrium nature of the experimental glass: since chaos is an *equilibrium* property, it is not clear how to detect it in non-equilibrium responses (such as the aging magnetic susceptibility [7], for instance). Nevertheless, TC is often regarded as the origin of the anomalous response of glasses in temperature cycles, and in particular, of the spectacular rejuvenation (and memory) effects found in SG [8] (however, see [9,10] for a dissenting view). Although memory and rejuvenation have been also identified in colloids [11], polymers [12,13], ferro-electrics [14,15], and in the ferromagnetic phase of disordered magnetic alloys [16], these are tiny effects as compared to their SG counterpart. Thus, experiments suggest that TC is peculiar in SG.

Unfortunately, a rigorous theoretical description of TC has been achieved only for directed polymers in random media in 1+1 dimensions [4,5]. Coming to SG, the analytical work has been mostly concerned with mean-field (MF) approximations. Some accidental cancellations make TC anomalously weak in the Sherrington-Kirkpatrick model [17] (the standard model in MF approximations), which favored a long controversy about its very existence [18–25]. Only recently the question has been answered in the positive, by the explicit computation of a large-deviation functional (*i.e.* the free-energy cost of constraining a SG to have similar spin configurations at two temperatures below the critical one, $T_1, T_2 < T_c$) [25,26]. A large-deviation functional will play as well a crucial role in this work.

Besides, the theoretical work in non-MF models is restricted to *equilibrium* numerical simulations [27–31]. Data were analyzed using a scaling picture (valid for polymers), in which a characteristic length scale should appear $\xi_C(T_1, T_2)$ in the comparison of the system at two temperatures $T_1, T_2 < T_c$ [32,33]. Spin configurations at temperatures T_1 and T_2 would be similar (different), if compared on length scales smaller (larger) than $\xi_C(T_1, T_2)$. The chaos length should diverge when T_1 approaches T_2 as $\xi_C \propto |T_2 - T_1|^{-1/\zeta}$. The numerical evidence for this picture is rather weak, which has been attributed to a large $\xi_C(T_1, T_2)$, comparable to or larger than the simulated system sizes [34]. Overall, the emerging picture is that of a gradual and extremely weak phenomenon.

However, the situation is murkier than suggested by the scaling picture. In the weak-chaos scenario [4] TC is almost absent in small systems with the exception of very

rare samples which are dramatically affected by small temperature changes. Weak chaos in SG has been reported in numerics [31], but a quantitative treatment in the infinite volume is lacking. Furthermore, we show below that the standard statistical analysis sweeps under the rug these very few chaotic samples.

Here, TC in three-dimensional SG is *quantitatively* treated as a rare-event–driven phenomenon. When TC occurs its effects are strong and can be felt even at the shortest length scales (which contradicts the common belief of a very long chaotic length). Finite-size effects are central to our approach because finite-size/time scaling is our only bridge between theoretical equilibrium computations (obtained for finite *sizes*), and the non-equilibrium responses accessible to experiment (at finite *times*) [35–38]. We achieve here the characterization of equilibrium TC and of its system size dependence, thus paving the way for the analysis of temperature cycles. Data suggest that naive dimensional analysis breaks down: the chaotic length diverges with system size L as $\xi_{\rm C}(T_1,T_2) \propto L^a\, a \approx 0.4$ (hence, $1 \ll \xi_{\rm C}(T_1,T_2) \ll L$ for large L). Two ingredients were crucial in this work. First, the Janus computer [39,40] gave us access to unprecedentedly large configurations, well thermalized up to very low temperatures [36,37]. Second, we introduce new tools of statistical analysis, based on a large-deviations functional.

In this work, we reanalyze Janus' equilibrium spin configurations already used in [36,37] for the $D = 3$ Edwards-Anderson model [41,42]. We consider Ising spins $s_{\mathbf{x}} = \pm 1$, each placed in the $V = L^D$ nodes $\mathbf{x}$ of a cubic lattice of linear size L, with periodic boundary conditions. The interaction is restricted to lattice nearest neighbors. The coupling constants $J_{\mathbf{x},\mathbf{y}} = \pm 1$ are chosen with 50% probability. This model undergoes a SG transition at $T_{\rm c} = 1.109(10)$ [43]. We study 4000 realizations of disorder, named *samples*, for $L = 8$, 12, 16 and 24 (1000 samples for $L = 32$). The minimal temperature in the Parallel Tempering simulation increased with L (for $L = 32$ it was $T_{\rm min} = 0.7026$).

Given the aforementioned difficulties on numerical investigations, it is crucial to chose wisely the quantities to be studied. Analytical approaches [25,26] suggest the study of the probability distribution function of the overlap between the spin configurations at temperatures T_1 and T_2,

$$q_{T_1,T_2} = \frac{1}{V}\sum_{\mathbf{x}} q_{\mathbf{x}}^{T_1,T_2}, \quad \text{with} \quad q_{\mathbf{x}}^{T_1,T_2} = s_{\mathbf{x}}^{T_1} s_{\mathbf{x}}^{T_2}, \qquad (1)$$

or alternatively, a similar extension of the link overlap,

$$Q_{T_1,T_2}^{\rm link} = \frac{1}{3V}\sum_{\|\mathbf{x}-\mathbf{y}\|=1} q_{\mathbf{x}}^{T_1,T_2} q_{\mathbf{y}}^{T_1,T_2}, \qquad (2)$$

where the summation is restricted to lattice nearest-neighbors (it has been argued that the link overlap is the relevant order parameter below the upper critical dimension [44,45]).

However, within the reachable system sizes, the spin overlap is not up to the task for numerical simulations [23]. Rather, finite-size effects are expected to be partly absorbed by a slight modification, the *chaotic parameter* [27]:

$$X_{T_1,T_2}^J = \left\langle q_{T_1,T_2}^2 \right\rangle_J \Big/ \left(\left\langle q_{T_1,T_1}^2 \right\rangle_J \left\langle q_{T_2,T_2}^2 \right\rangle_J \right)^{1/2}. \qquad (3)$$

Here, $\langle\cdot\rangle_J$ refers to thermal averages within the same sample. Note that $0 < X_{T_1,T_2}^J \leq 1$. In fact, X_{T_1,T_2}^J is similar to a correlation parameter ($X_{T_1,T_2}^J = 1$ means that, for that particular sample, typical spin configurations at T_1 and T_2 are indistinguishable, while $X_{T_1,T_2}^J = 0$ indicates extreme chaos). However, the standard analysis of X_{T_1,T_2}^J (wrongly) concluded that chaos was very weak. For later reference, we remark that the chaotic parameter can be generalized to the link overlap

$$X_{T_1,T_2}^{{\rm link},J} = \left\langle Q_{T_1,T_2}^{\rm link} \right\rangle_J \Big/ \Big(\left\langle Q_{T_1,T_1}^{\rm link} \right\rangle_J \left\langle Q_{T_2,T_2}^{\rm link} \right\rangle_J \Big)^{1/2}. \qquad (4)$$

We shall see that $X_{T_1,T_2}^{{\rm link},J}$ is just as informative as X_{T_1,T_2}^J, as it could be expected from replica equivalence [36,45,46].

We need some new insight to find a good observable. Following [47,48], we will seek it in the Monte Carlo dynamics, specifically in the temperature flow of the Parallel Tempering [49,50]. Indeed, if the equilibrium configuration for two neighboring temperatures are too different (TC), a bottleneck in the temperature random-walk should appear. Now, the performance of Parallel Tempering deteriorates dramatically when the system size grows from $L = 8$ to $L = 32$ [36]. It follows that some strong form of TC is waiting to be unveiled.

The temperature flow dynamics is characterized by its exponential autocorrelation time, $\tau_{\rm exp}$ [36,51]. Note that $\tau_{\rm exp}$ is potentially unbounded, while X_{T_1,T_2}^J is limited within 0 and 1. Hence, $\tau_{\rm exp}$ should provide a clear flag signaling those samples that suffer strong chaos. It follows that the quantity that better correlates with $\log\tau_{\rm exp}$ will also be the most informative about chaos. After some failures [52], we found strong anticorrelation with the integral of X_{T_1,T_2}^J with T_2, $I = \int_{T_1}^{T_{\rm max}} X_{T_1,T_2}^J {\rm d}T_2$, see fig. 1. If X_{T_1,T_2}^J suffers a sharp drop at low T_2 (thus making the integral I small), the temperature flow in that sample is likely to get stuck. These samples are completely neglected by the standard statistical analysis.

Figure 2 describes the necessary change of paradigm. The top panel shows the standard average over the samples of X_{T_1,T_2}^J, as a function of T_2. In agreement with previous work [27,28,31], our simulated sizes are painfully away from the large-L limit, where the average of X_{T_1,T_2}^J should vanish if $T_2 \neq T_1$. Instead, our curves are smooth and cross $T_{\rm c}$ without qualitative changes. Yet, the behavior of individual samples is quite different, fig. 2, center. At well-defined temperatures T_2, X_{T_1,T_2}^J falls abruptly for some samples. This we name *chaotic event*. The temperature at which these events occur is random (many samples do not suffer any). In fact, as L grows, the sample dispersion of X_{T_1,T_2}^J reaches a maximum in the SG phase.

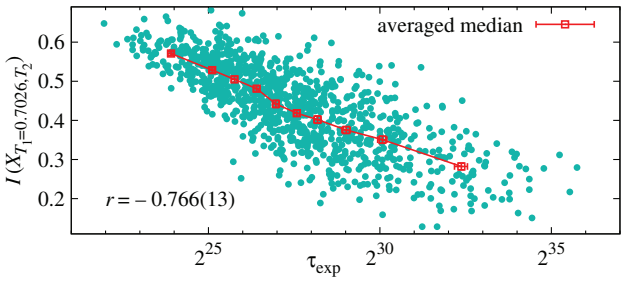

Fig. 1: (Color online) Seeking clues about TC on the parallel tempering autocorrelation time $\tau_{\rm exp}$ [36]. For each sample we show I *vs.* $\log\tau_{\rm exp}$, where $I = \int_{T_1}^{T_{\rm max}} X^J_{T_1,T_2}\mathrm{d}T_2$ and $X^J_{T_1,T_2}$ is defined in eq. (3) ($T_1 = T_{\rm min} = 0.7026$, $T_{\rm max} = 1.549$, data for $L = 32$). The correlation parameter r is computed with $\log\tau_{\rm exp}$ due to the wild sample-to-sample fluctuations of $\tau_{\rm exp}$. The red line was computed by a delicate procedure: we ordered the samples by increasing $\log\tau_{\rm exp}$ and made groups of 100 consecutive samples; within each group, medians were computed (errors from bootstrap).

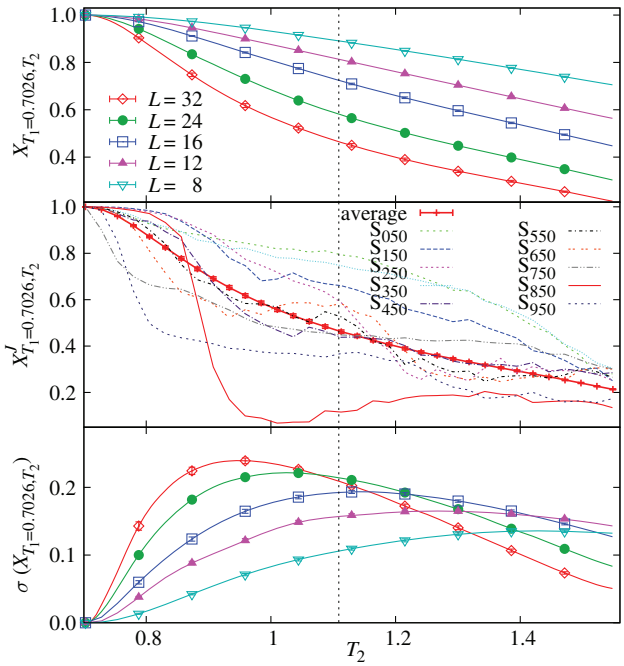

Fig. 2: (Color online) Different views on $X^J_{T_1,T_2}$, eq. (3), as function of T_2 ($T_1 = 0.7026$, the vertical line is $T_2 = T_{\rm c}$). Top: for all our system sizes, sample-average of $X^J_{T_1,T_2}$. Center: for $L = 32$, we show $X^J_{T_1,T_2}$ for ten samples evenly spaced on a list of growing $\tau_{\rm exp}$, recall fig. 1. Bottom: for all our system sizes, we show the dispersion (*i.e.* square root of variance over the samples) of $X^J_{T_1,T_2}$.

This is the first time that a clear difference between the paramagnetic and the SG phase is observed when studying $X^J_{T_1,T_2}$. We conclude that the full probability distribution of $X^J_{T_1,T_2}$ should be studied.

A natural question arises at this point. The link overlap carries information only at distance one, supposedly much

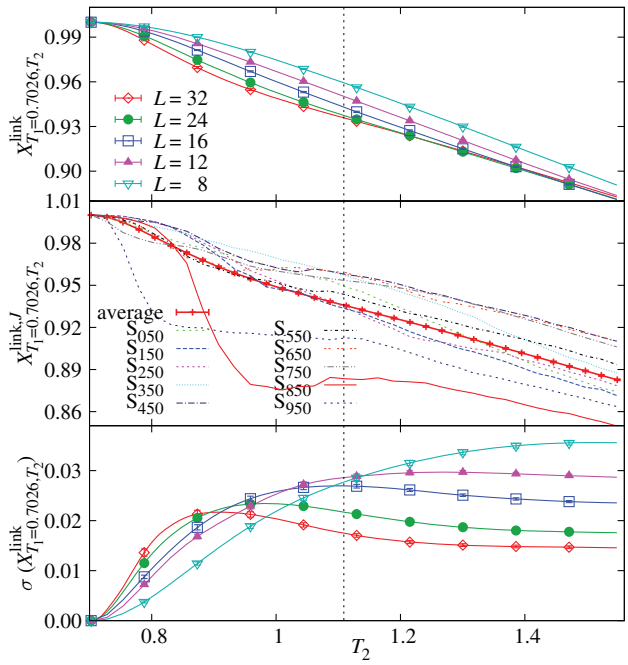

Fig. 3: (Color online) Same analysis as in fig. 2, carried out with the link overlap $X^{{\rm link},J}_{T_1,T_2}$, see eq. (4).

smaller than the chaos length $\xi_{\rm C}(T_1,T_2)$ [34]. Can it carry as much information as the spin overlap, as expected from overlap equivalence considerations? The answer is *yes*, see fig. 3 where we compare the spin and link chaotic parameters. Indeed, the chaotic events observed in certain samples in fig. 2, center, appear just as clearly for the very same samples in fig. 3, center. We will come back to this point below when we discuss the spatial correlation function (in fact, the link overlap is a correlation function at distance one).

We now consider the probability distribution of $X^J_{T_1,T_2}$. The fraction of samples that suffer a chaotic event for any pair of temperatures T_1, T_2 ($T_1 < T_2 < T_{\rm c}$) increases with L, see fig. 4, top. The statement is made quantitative by introducing a large-deviation potential $\Omega^L_{T_1,T_2}(\varepsilon)$ [25,26]:

$$\text{Probability}[X^J_{T_1,T_2} > \varepsilon] = \mathrm{e}^{-L^D\Omega^L_{T_1,T_2}(\varepsilon)}. \qquad (5)$$

Several comments are in order:

- A large-deviation potential is useful only if $\Omega^L_{T_1,T_2}(\varepsilon)$ becomes L-independent for moderate system sizes. This happens for $L = 24$ and 32 in fig. 4, bottom (see [52] for other pairs of temperatures).
- $\Omega_{T_1,T_2}(\varepsilon)$ contains all the information on finite-size scaling. The values of $X^J_{T_1,T_2}$ that are likely on samples of size L are such that $L^D\Omega_{T_1,T_2}(X^J_{T_1,T_2}) \sim 1$. This results in a power-law scaling, see eq. (6) below.
- If $\Omega_{T_1,T_2}(\varepsilon)$ remains positive for large L and all $\varepsilon > 0$, the probability of *not* finding a chaotic sample is exponentially small in L^D.

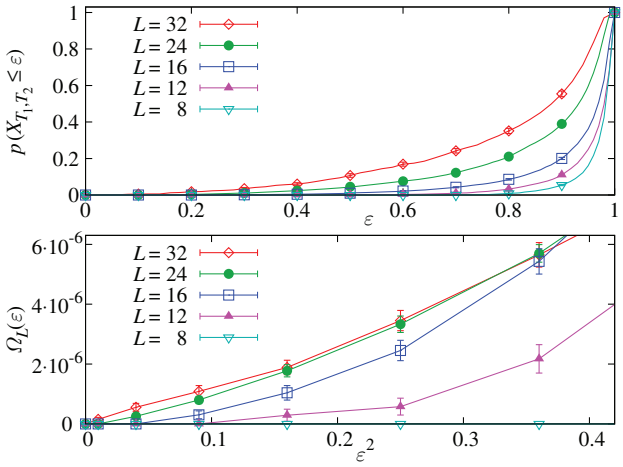

Fig. 4: (Color online) Top: probability of finding $X^J_{T_1,T_2} \le \varepsilon$ as a function of ε, for temperatures $T_1 = 0.7026$ and $T_2 = 0.83923$ and all our system sizes. Bottom: large-deviation potential, eq. (5), as a function of ε^2, from data in the top panel (for other T_1, T_2, see [52]). Chaos is absent for $L = 8$, since Ω_{T_1,T_2} is essentially zero. Ω_{T_1,T_2} increases as L grows, reaching a limiting behavior for $L = 24$.

– $\Omega_{T_1,T_2}(\varepsilon)$ can also be read as an ε-dependent length scale $\sim 1/\Omega^{1/D}_{T_1,T_2}(\varepsilon)$. This is *not* the chaotic length of the scaling picture [4,32,33], which is ε-*independent.*

Chaos should weaken when T_2 approaches T_1. In fact, MF [26] suggests the following scaling for the large-deviation potential, in the limit $L \to \infty$, for small ε and $|T_1 - T_2|$:

$$\Omega_{T_1,T_2}(\varepsilon) \propto |T_1 - T_2|^b \varepsilon^\beta. \qquad (6)$$

Our data for fixed $|T_1 - T_2|$ suggest $\beta \approx 1.7$, see fig. 4, bottom and [52]. Hence, $\Omega_{T_1,T_2}(\varepsilon) > 0$ for all $\varepsilon > 0$: the existence of TC is established.

The exponent $\beta \approx 1.7$ in eq. (6) has some consequences. To discuss them, it is enlightening to consider the spatial correlation function for temperatures T_1 and T_2:

$$C^J_{T_1,T_2}(r) = \frac{1}{3V} \sum_{\mathbf{r};|\mathbf{r}|=r} \sum_{\mathbf{x}} \left\langle s^{T_1}_{\mathbf{x}} s^{T_2}_{\mathbf{x}} s^{T_1}_{\mathbf{x}+\mathbf{r}} s^{T_2}_{\mathbf{x}+\mathbf{r}} \right\rangle_J . \qquad (7)$$

Now we average this function separately over the 10% most (less) chaotic samples[1], as well as the totality of them, as shown in fig. 5. The behavior of the chaotic samples is qualitatively different, as shown by the correlation-length ξ. On non-chaotic samples, we get $\xi_{\rm NC} \approx L/2$ while, for the chaotic $L = 32$ samples we obtain $\xi_{\rm C} \approx 6$ for $L = 32$. As announced in the discussion of eq. (5), an analysis based on a *single* chaotic length [32,33] is incomplete.

The natural question, now, is how $\xi_{\rm C}$ behaves when L grows *for the typical samples* (*i.e.* those with $X^J_{T_1,T_2}$ such

[1]In $L = 32$, the 10% most (less) chaotic samples are given by the samples that fulfill $X_{T_1,T_2} \le 0.33$ ($X_{T_1,T_2} > 0.93$). We keep the same X_{T_1,T_2}-thresholds for $L = 24$.

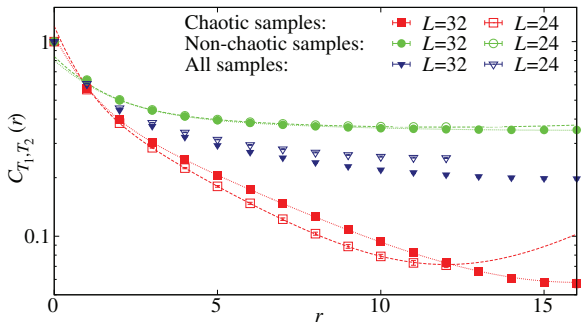

Fig. 5: (Color online) Spatial correlation function for $T_1 = 0.70260$ and $T_2 = 0.90318$, eq. (7), as averaged over different sets of samples: all samples, non-chaotic samples ($X_{T_1,T_2} > 0.93$) and chaotic samples ($X_{T_1,T_2} \le 0.33$). Lines are fits to $\sum_{i=1,2} A_i \left(e^{-x/\xi_i} + e^{-(L-x)/\xi_i}\right)$. For each fit, the largest correlation lengths were $\xi^{L=32}_{\rm chaos} = 5.69(2)$, $\xi^{L=24}_{\rm chaos} = 4.447(15)$, $\xi^{L=32}_{\rm non\text{-}chaos} = 23.7(7)$, $\xi^{L=24}_{\rm non\text{-}chaos} = 18.9(3)$.

that $L^D \Omega_{T_1,T_2} \sim 1$). Equation (6) provides a shocking answer: $\xi_{\rm C} \sim L^a$, with $a = (\beta - 1)/\beta$ (see footnote [2]). Our numerical results indicate that $a \approx 0.4$, so that ξ_C diverges with L.

Actually, only $\beta = 1$ in eq. (6) would be compatible with a finite $\xi_{\rm C}$. However, we cannot neglect this possibility. Indeed, the MF computation [26] warns us that eq. (6) is probably only the leading order in an expansion in ϵ and $|T_1 - T_2|$. Further, subleading terms should be expected. They would cause transient effects for small systems[3]. In fact, the positive curvature that appears for large ϵ in fig. 4, bottom is probably due to these contributions (subleading for small ε). Thus, the scaling displayed in fig. 4 could be still pre-asymptotic.

But, if the chaotic length coming from the scaling picture cannot be given a meaning (because the system sizes

[2]Indeed, barring normalizations, $\langle q^2_{T_1,T_2}\rangle_J$ is the space integral of the correlation function (7), recall eq. (1). It follows that $\langle q^2_{T_1,T_2}\rangle_J \propto (\xi_{\rm C}/L)^D$. Since below $T_{\rm c}$, both $\langle q^2_{T_1,T_1}\rangle_J$ and $\langle q^2_{T_2,T_2}\rangle_J$ are of order one, also $X^J_{T_1,T_2} \sim (\xi_{\rm C}/L)^D$. Now, plug eq. (6) with $\beta \approx 2$ in eq. (5). If the probability in eq. (5) is to remain of order one for large L, then $X^J_{T_1,T_2} \sim 1/L^{D/\beta}$. But $X^J_{T_1,T_2} \sim (\xi_{\rm C}/L)^D$, so $\xi_{\rm C} \sim L^a$, with $a = (\beta - 1)/\beta \approx 0.4$. The conclusion does not change if we consider an algebraically decaying prefactor, $C^J_{T_1,T_2}(r) \sim \exp[-r/\xi_{\rm C}]/r^c$ for large r [9]. In such case, $\langle q^2_{T_1,T_2}\rangle_J \propto \xi_{\rm C}^{D-c}/L^D$ and $\xi_{\rm C} \sim L^{D(\beta-1)/(\beta(D-c))}$ (but our data suggest $c \approx 0$, $\beta \approx 1.7$). Furthermore, if for sizes $L > 32$ one had $\beta = 1$ (so that $\xi_{\rm C}$ would be finite for large L), then $\xi_{\rm C} \sim |T_1 - T_2|^{-b/(D-c)}$.

[3]In fact, in MF [26], for small overlap and $|T_1 - T_2|$, the large-deviations potential scales as

$$\tilde{\Omega}^{\text{mean-field}} \propto A q^2_{T_1,T_2} |T_1 - T_2|^3 + B |q_{T_1,T_2}|^3 |T_1 - T_2|^2,$$

(A and B are constants). Either of the two terms can be dominant for some region of q, N and $T_1 - T_2$ (N is the number of spins). We now let N grow at fixed $T_1 - T_2$, and seek q such that $\tilde{\Omega} \sim 1/N$ (*i.e.* probability of order one, see eq. (5)). We realize that there is a crossover size $N^* \sim |T_1 - T_2|^{-5}$ such that $q^2 \sim N^{-2/3}$ if $N \ll N^*$. On the other hand, if $N \gg N^*$, $q^2 \sim N^{-1}$: the MF prediction for eq. (6) is $\beta = 1$.

available to current simulation yield $\beta \approx 1.7$, *i.e.* an infinite ξ_C), what is the chaos exponent ζ computed in previous work [30,31]? (recall that, supposedly, $\xi_C \propto |T_2 - T_1|^{-1/\zeta}$). In fact, the chaos exponent ζ was computed indirectly, through phenomenological renormalization [3] ($\zeta \approx 1.07$ in $D = 3$ [31] and $\zeta \approx 1.12$ in $D = 4$ [30]). We will now argue that this exponent is actually $\zeta = D/b$ (b is the temperature difference exponent in eq. (6)). So, ζ is unrelated to the chaos length.

Indeed, some reflection reveals that phenomenological renormalization [31] can be cast as follows. For the purpose of discussion, fix the lowest temperature T_1. Then, for each L, find a $T_2(L)$ such that the probability distribution function for $X^J_{T_1,T_2(L)}$, becomes L-independent, see fig. 6, top. The exponent ζ of ref. [31] follows from $L \propto 1/|T_1 - T_2(L)|^{1/\zeta}$, see fig. 6, bottom[4]. But, combining eqs. (5) and (6), one realizes that phenomenological renormalization amounts to the statement $L^D |T_1 - T_2(L)|^b \sim 1$, which implies $\zeta = D/b$.

The computation of ζ from eq. (6) is reported in fig. 6, center. There seems to be two scaling regimes. For small temperature differences, the regime where eq. (6) applies, we find $b = 2.81(13)$, or $\zeta = 1.07(5)$, in excellent agreement with [31]. We note, however, that this b value applies only when $|T_1 - T_2(L)| < 0.25$, when chaotic events are rather rare for our system sizes. As anticipated in the Introduction, we see that the standard statistical analysis is blind to TC.

It is time for some interpretation. We have introduced the concept of a chaotic event. Such chaotic events are pretty much similar to a "level crossing" in Quantum Mechanics: at some specific temperature a new state becomes favorable and takes over the old one. This is consistent with the fact that chaotic events are noticeable even at distance one, see fig. 3. Now, our data suggest that, in the large L limit and for any two temperatures $T_1, T_2 < T_c$ one should find a chaotic event with probability one. Hence, given any pair of temperatures $T_a < T_b$, one may consider a sequence $T_a < T_1 < T_2 < T_3 < \cdots < T_N < T_b$. Chaotic events should appear in any subinterval $[T_i, T_{i+1}]$. It is clear that a large amount of level crossings between temperatures $T_a < T_b$ can only result on the vanishing of the spin overlap for both temperatures. This picture bears some similarities to the findings within Migdal-Kadanoff renormalization [53], where a positive Lyapunov exponent guarantee the vanishing of the spin overlap (we remark that the positive Lyapunov exponent appears within this approach for a large variety of models, both regarding the spin type and the coupling distribution).

In summary, we have *quantitatively* characterized TC in the $D = 3$ Ising SG as a rare-event–driven phenomenon, inaccessible to the statistical analysis employed in previous work. Instead, we perform a large-deviations analysis of the Janus equilibrium configurations (remarkable both for system sizes up to $L = 32$ and for the low temperatures). The large deviation functional characterize the size dependences, a crucial step towards the extension of time-length dictionaries for temperature-varying experimental protocols. A surprising outcome is that the chaotic length scales with system size as $\xi_C \propto L^a$, with $a \approx 0.4$: divergent in the thermodynamic limit, yet much smaller than L. This duality will probably be important to interpret the somehow contradictory memory and rejuvenation effects. In fact, although the $\xi_C \propto L^a$ scaling follows from a $L \to \infty$ extrapolation (which is tricky even in MF), we now know that a meaningful comparison with experiments requires only an extrapolation to $L \sim 110$ lattice spacings [36].

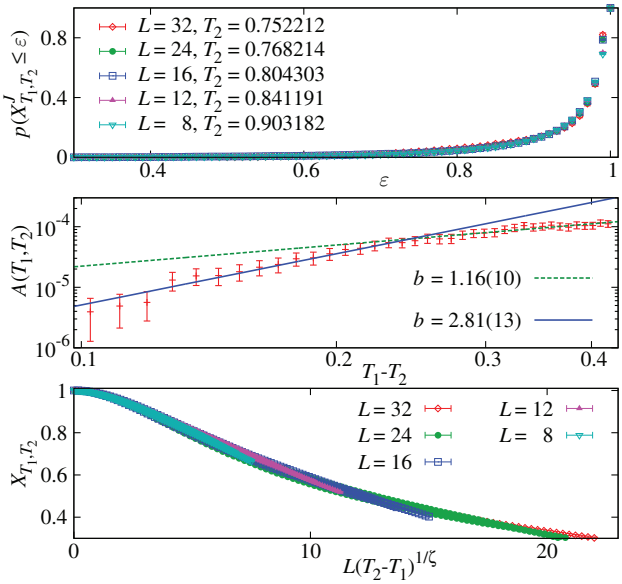

Fig. 6: (Color online) Top: phenomenological renormalization: for each L, we seek $T_2(L)$ such that the distribution function $p\big(X^J_{T_1=0.7026,T_2(L)} \le \varepsilon\big)$ best resembles the $L = 8$ distribution for $T_1 = 0.7026$ and $T_2 = 0.90318$. Middle: computation of exponent b in eq. (6). First, we fit to $\Omega^{L=32}_{T_1,T_2}(\varepsilon) = A(T_1,T_2)\varepsilon^2 + B(T_1,T_2)\varepsilon^4$. We show $A(T_1,T_2)$ *vs.* $T_1 - T_2$, and two power-law fits. Bottom: sample-averaged $X^J_{T_1,T_2}$ *vs.* $L(T_1 - T_2)^{1/\zeta}$ using $\zeta = 1.06$ (data for $T_1 = 0.7026$ and, when $L \le 24$, also for $T_2 = 0.625$). Unfortunately, data collapse both for $T_2 < T_c$ and for T_2 in the paramagnetic phase (see also [53]).

* * *

We are indebted with the Janus Collaboration for allowing us to analyze their thermalized configurations. We thank particularly David Yllanes for discussions and for assistance in the data analysis. We acknowledge support from MINECO, Spain, through research contracts FIS2012-35719-C02 and from the European Research Council (ERC) through grant agreement No. 247328. BS was supported by the FPU program (MECD, Spain).

[4] A fit to $T_1 - T_2(L) \propto 1/L^\zeta$ yields $\zeta = 1.02(3)$ (for $L \le 32$, $T_1 = 0.7026$ and $T_2(L = 8) = 0.90318$, with $\chi^2/\text{dof} = 3.57/3$) or $\zeta = 1.07(2)$ (for $L \le 24$, $T_1 = 0.625$ and $T_2(L = 8) = 0.815$, with $\chi^2/\text{dof} = 1.77/2$). These results can be compared with $\zeta \approx 1.07$ [31].

REFERENCES

[1] McKay S. R., Berker A. N. and Kirkpatrick S., *Phys. Rev. Lett.*, **48** (1982) 767.
[2] Bray A. J. and Moore M. A., *Phys. Rev. Lett.*, **58** (1987) 57.
[3] Banavar J. R. and Bray A. J., *Phys. Rev. B*, **35** (1987) 8888.
[4] Sales M. and Yoshino H., *Phys. Rev. E*, **65** (2002) 066131.
[5] da Silveira R. A. and Bouchaud J.-P., *Phys. Rev. Lett.*, **93** (2004) 015901.
[6] Cieplak M., Li M. S. and Banavar J. R., *Phys. Rev. B*, **47** (1993) 5022.
[7] Vincent E. *et al.*, *Slow dynamics and aging in spin glasses*, in *Complex Behavior of Glassy Systems*, edited by Rubí M. and Pérez-Vicente C., *Lect. Notes Phys.*, Vol. **492** (Springer, Berlin) 1997.
[8] Jonason K. *et al.*, *Phys. Rev. Lett.*, **81** (1998) 3243.
[9] Berthier L. and Bouchaud J.-P., *Phys. Rev. B*, **66** (2002) 054404.
[10] Berthier L. and Bouchaud J.-P., *Phys. Rev. Lett.*, **90** (2003) 059701.
[11] Ozon F. *et al.*, *Phys. Rev. E*, **68** (2003) 032401.
[12] Bellon L., Ciliberto S. and Laroche C., *Europhys. Lett.*, **51** (2000) 551.
[13] Yardimci H. and Leheny R. L., *Europhys. Lett.*, **62** (2003) 203.
[14] Bouchaud J.-P., Doussineau P., de Lacerda-Arôso T. and Levelut A., *Eur. Phys. J. B*, **21** (2001) 335.
[15] Mueller V. and Shchur Y., *Europhys. Lett.*, **65** (2004) 137.
[16] Vincent E. *et al.*, *Europhys. Lett.*, **50** (2000) 674.
[17] Sherrington D. and Kirkpatrick S., *Phys. Rev. Lett.*, **35** (1975) 1792.
[18] Kondor I., *J. Phys. A*, **22** (1989) L163.
[19] Kondor I. and Végsö, *J. Phys. A*, **26** (1993) L641.
[20] Billoire A. and Marinari E., *J. Phys. A*, **33** (2000) L265.
[21] Rizzo T., *J. Phys.*, **34** (2001) 5531.
[22] Mulet R., Pagnani A. and Parisi G., *Phys. Rev. B*, **63** (2001) 184438.
[23] Billoire A. and Marinari E., *Europhys. Lett.*, **60** (2002) 775.
[24] Krzakala F. and Martin O. C., *Eur. Phys. J. B*, **28** (2002) 199.
[25] Rizzo T. and Crisanti A., *Phys. Rev. Lett.*, **90** (2003) 137201.
[26] Parisi G. and Rizzo T., *J. Phys. A*, **43** (2010) 235003.
[27] Ney-Nifle M. and Young A., *J. Phys. A*, **30** (1997) 5311.
[28] Ney-Nifle M., *Phys. Rev. B*, **57** (1998) 492.
[29] Krzakala F., *Europhys. Lett.*, **66** (2004) 847.
[30] Sasaki M., Hukushima K., Yoshino H. and Takayama H., *Phys. Rev. Lett.*, **95** (2005) 267203.
[31] Katzgraber H. G. and Krzakala F., *Phys. Rev. Lett.*, **98** (2007) 017201.
[32] Fisher D. S. and Huse D. A., *Phys. Rev. Lett.*, **56** (1986) 1601.
[33] Bray A. J. and Moore M. A., *Scaling theory of the ordered phase of spin glasses*, in *Heidelberg Colloquium on Glassy Dynamics*, edited by van Hemmen J. L. and Morgenstern I., *Lect. Notes Phys.*, Vol. **295** (Springer, Berlin) 1987.
[34] Aspelmeier T., Bray A. J. and Moore M. A., *Phys. Rev. Lett.*, **89** (2002) 197202.
[35] Franz S., Mézard M., Parisi G. and Peliti L., *Phys. Rev. Lett.*, **81** (1998) 1758.
[36] Álvarez Baños R. *et al.*, *J. Stat. Mech.* (2010) P06026.
[37] Álvarez Baños R. *et al.*, *Phys. Rev. Lett.*, **105** (2010) 177202.
[38] Barrat A. and Berthier L., *Phys. Rev. Lett.*, **87** (2001) 087204.
[39] Belletti F. *et al.*, *Comput. Phys. Commun.*, **178** (2008) 208.
[40] Belletti F. *et al.*, *Comput. Sci. Eng.*, **11** (2009) 48.
[41] Edwards S. F. and Anderson P. W., *J. Phys. F*, **5** (1975) 965.
[42] Edwards S. F. and Anderson P. W., *J. Phys. F*, **6** (1976) 1927.
[43] Hasenbusch M., Pelissetto A. and Vicari E., *Phys. Rev. B*, **78** (2008) 214205.
[44] Contucci P., *J. Phys. A: Math. Gen.*, **36** (2003) 10961.
[45] Contucci P., Giardinà C., Giberti C. and Vernia C., *Phys. Rev. Lett.*, **96** (2006) 217204.
[46] Parisi G. and Ricci-Tersenghi F., *J. Phys. A: Math. Gen.*, **33** (2000) 113.
[47] Schulman L. S., *Phys. Rev. Lett.*, **98** (2007) 257202.
[48] Fernandez L. A., Martin-Mayor V. and Verrocchio P., *Phys. Rev. E*, **73** (2006) 020501.
[49] Hukushima K. and Nemoto K., *J. Phys. Soc. Jpn.*, **65** (1996) 1604.
[50] Marinari E., *Optimized Monte Carlo methods*, in *Advances in Computer Simulation*, edited by Kerstész J. and Kondor I. (Springer-Verlag) 1998.
[51] Sokal A. D., *Monte Carlo methods in statistical mechanics: Foundations and new algorithms*, in *Functional Integration: Basics and Applications (1996 Cargèse School)*, edited by DeWitt-Morette C., Cartier P. and Folacci A. (Plenum, New York) 1997.
[52] Seoane B., PhD Thesis (Universidad Complutense de Madrid) 2013, `http://arxiv.org/abs/1309.2269`.
[53] Ilker E. and Nihat Berker A., *Phys. Rev. E*, **87** (2013) 032124.